RECENT EXPERIMENTAL STUDIES OF CONTINUOUS TRANSFORMATIONS IN ALLOYS: AN OVERVIEW

W. A. Soffa* and D. E. Laughlin**
*Department of Metallurgical & Materials Engineering
University of Pittsburgh
Pittsburgh, PA 15261
**Department of Metallurgical Engineering & Materials Science
Carnegie-Mellon University
Pittsburgh, PA 15213

Over the past decade a unified view of spinodal decomposition and continuous ordering processes has evolved, and this generalized perspective has substantially clarified the nature of order-disorder reactions in alloys, and the interplay of ordering and clustering in precipitation systems. The concept of concentration waves and the reciprocal lattice approach provide the foundation of this modern view of continuous phase transformations. Herein, these concepts are combined with free energy-composition and phase diagrams to survey systematically and interpret a number of selected studies of transformations occurring in metallic solid solutions. Observations and data obtained by a variety of experimental methods including X-ray and electron diffraction, transmission electron microscopy (TEM) and atom probe field-ion microscopy (APFIM) are critically examined. From this overview a framework is constructed which provides a means for classifying different types and combinations of diffusional instabilities involving long and/or short wavelength concentration waves giving rise to phase separation and/or ordering in binary and ternary systems.

J. Willard Gibbs (1) distinguished between two fundamental modes of transformations which may occur in physical systems; namely, (i) those transformations which are initiated by fluctuations that are large in degree and small in extent (e.g., classical nucleation) and (ii) those which are initiated by fluctuations that are small in degree and large in extent (e.g., spinodal decomposition). In the same vein, J. W. Christian (2) distinguishes between heterogeneous and homogeneous transformations. Heterogeneous transformations, which include both classical homogeneous and heterogeneous nucleation processes, generally involve the spatial partitioning of the system into regions which are transformed and regions which are untransformed, separated by interphase interfaces. Homogeneous transformations are those in which the transformation occurs uniformly throughout the entire ensemble and the composition and/or the order parameter are progressively increased from initially small values to large values characteristic of a more stable state. The latter can be called <u>continuous transformation</u> since the entire system transforms <u>via</u> the "continuous" amplification of initially small fluctuations within the supersaturated or undercooled phase.

In this paper, we shall review selected experimental evidence characterizing continuous transformations occurring in the metallic solid state. We shall limit the study to those continuous transformations which involve diffusional instabilities with respect to long and/or short wavelength quasi-periodic fluctuations within supersaturated solid solutions and ordering systems. No attempt will be made to review non-diffusional instabilities such as those associated with displacive transformations (e.g., ω phase).

Several limiting cases of diffusional continuous phase transformations exist. For example, at sufficient undercoolings long wavelength quasi-periodic fluctuations may occur in systems that exhibit a simple miscibility gap. Such a reaction is usually termed "spinodal decomposition" (3). The original single-phase alloy decomposes into a metastable coherent two-phase mixture in which spatial periodicity is generally evident. Furthermore, in an elastically anisotropic matrix in which coherency strains develop, crystallographic alignment of the two phases is expected (4). At the small wavelength end of the fluctuation spectrum (c. 5 Å) continuous processes occur which produce ordered atomic arrays. These have been classified as either "continuous ordering" or "spinodal ordering" (5). Finally, clustering and ordering may occur in sequence or concomitantly. If in sequence, the long wavelength clustering reaction may either precede or follow the development of the short wavelength ordering reaction (6-10).

In this review, we shall discuss each of the above phase transformations from the point of view of free energy curves, phase diagrams, concentration waves and reciprocal space, and review experimental observations in a variety of alloys. Importantly, we hope to provide not only a compilation of results, but also to present a framework in which the complex spectrum of interplay between clustering and ordering in precipitation systems can be classified systematically and understood.

Concentration Waves and the Reciprocal Lattice Approach

The concept of concentration waves was first emphasized as an important tool for understanding transformations in metallic solid solutions in the works of Hillert (11,12) and Cahn (3,13) and later developed and generalized by de Fontaine, Cook and Hilliard (5,14,15). The latter approach focuses on a discrete lattice method used extensively by Krivoglaz (16) and Khachaturyan (17) in the Russian literature and is generally applicable to the early stages of continuous transformations. The discrete lattice formalism contains the continuum theory of Cahn describing spinodal decomposition as the long wavelength limit and also provides a basis for describing both first and second-order (higher order) continuous ordering transitions. Since the construct of concentration waves plays a central role in the systematic description of continuous phase transformations it is deemed appropriate here to provide a brief elementary overview of this notion as it is used to characterize fluctuations and diffusional instabilities in solid solutions. The discussion follows essentially the approach promulgated by de Fontaine (5) since this perspective provides a rather straightforward tool for understanding the complex interplay of clustering and ordering often occurring in precipitation systems.

The atomic arrangements or composition fluctuations characterizing a solid solution can be considered as a superposition of simple cosinusoidal waves of various amplitudes and wavelengths along specific crystallographic directions. This spectrum of concentration waves defining the distribution of atoms over the lattice sites simply represents the Fourier components of the concentration variables. The localization of the components or "normal

modes" of the atomic configuration at specific points in the first Brillouin zone is particularly useful for understanding the various diffuse scattering effects which accompany clustering and ordering; the scattered amplitude at a location in the reciprocal lattice is proportional to the amplitude of the corresponding Fourier component of the composition function describing the heterogeneities in real space.

Using a general Bragg-Williams model the excess free energy of a solid solution can be represented in the harmonic approximation in reciprocal space by the expression (5)

$$\Delta F \equiv F_M - F_o = \frac{N}{2} \sum_{\vec{k}} F''(k) \left|X(k)\right|^2 \tag{1}$$

where F_M is the free energy of mixing and F_o is the free energy of mixing in the disordered state; $F''(k)$ is the Fourier transform of the second order term in the Taylor series expansion of the free energy about the disordered state; $|X(k)|^2$ is the square of the Fourier transform of the concentration variable $(c-\bar{c})$ or concentration deviation from the mean. The coefficient $F''(k)$ is given by

$$F''(k) = 2V(k) + \frac{k_B T}{\bar{c}(1-\bar{c})} \tag{2}$$

where $V(k)$ is the $\vec{k}$-space potential related to the Fourier transform of the effective pair interaction potential $V(r) = \frac{1}{2}[V_{AA}(r) + V_{BB}(r) - 2V_{AB}(r)]$. This excess free energy of the solid solution relative to the disordered state in the $\vec{k}$-space representation is essentially the sum of the free energies of the various concentration waves localized at the sites $\vec{k}$ in reciprocal space, and the contribution of a particular wave to the total free energy is proportional to the square of the amplitude of this Fourier component.

There is an intimate relationship between the behavior of composition fluctuations in solid solutions and the occurrence of diffusional instabilities at lower temperatures. In a single phase alloy above the transformation temperature the diffuse scattering resulting from composition fluctuations is given by

$$I_{SRO}(k) = \text{constant} \times \frac{k_B T}{\bar{c}(1-\bar{c})F''(k)} \tag{3}$$

where k_B is the Boltzmann constant, T is the absolute temperature, $\bar{c}$ is the average concentration, and $F''(k)$ is the harmonic free energy coefficient defined above. This is the well-known Krivoglaz (16) and Clapp-Moss (18,19) formula which derives from the expression for the expectation values of the amplitudes of dynamic composition fluctuations. At high temperatures and for small amplitudes the harmonic term is sufficient and higher order terms in the free-energy expansion can be neglected.

Diffusional instabilities associated with clustering and ordering occur when certain large amplitude fluctuations or concentration waves build up and become unbounded at the instability limit. Long wavelength clustering waves occur in the vicinity of (000), at the center of the first Brillouin zone, whereas ordering instabilities are usually expected at "special points" of fcc and bcc lattices where symmetry elements intersect and extrema of the $F''(k)$ occur, i.e., points where $V(k)$ is a minimum. Ordering instability occurs at temperature T_i for which the modulus $F''(k)$ vanishes. Thus, at T_i defined by

$$k_B T_i = -2\bar{c}(1-\bar{c})V(\vec{k}_o) \tag{4}$$

where $\vec{k}_o$ is a "special point" wave vector, e.g., $\langle 1\frac{1}{2}0\rangle$, the ordering wave $\vec{k}_o$ is amplified spontaneously initiating continuous decomposition of the parent phase. These "special point" instabilities represent the uppermost

instability limits or "ordering spinodals" (20).

For small amplitude fluctuations (the harmonic approximation) the kinetics of amplification of specific concentration waves is described by a simple exponential

$$X(k,t) = X(k,o)\ \exp[\alpha(k)t] \tag{5}$$

where the amplification factor $\alpha(k)$ is given by

$$\alpha(k) = -M\beta(k)F''(k) \tag{6}$$

in which M is an atomic mobility parameter and $\beta(k)$ is a geometrical factor depending on the disposition of nearest neighbors and the coordination. When the wave vector $\vec{k}$ is small (near the origin of the first Brillouin zone, i.e., the long wavelength limit), $\alpha(k)$ reduces to Cahn's amplification factor describing spinodal decomposition (21). It is important to note that the $\vec{k}$-space harmonic free energy contains both the gradient energy and elastic energy contributions to the total excess free energy. The kinetic law for amplification simply shows that waves with k-vectors corresponding to negative values of $\alpha(k)$ will tend to decay, whereas certain waves with positive values of $\alpha(k)$ will grow spontaneously; waves of maximum $\alpha(k)$ are expected to grow preferentially. It should be pointed out that below an instability limit, concentration waves corresponding to maxima in the kinetic $\alpha(k)$ may not always coincide with the "special point" waves associated with extrema in the V(k) function (5).

The picture that emerges can be summarized as follows: in the vicinity of an instability temperature large-amplitude fluctuations associated with specific concentration waves tend to appear. In the vicinity of a second-order (higher order) phase transition these dynamic fluctuations directly signal the approach to the transformation temperature since the transformation temperature and instability limit coincide; for first-order transitions the instability limit appears at temperatures below the phase boundary. At the instability limit selected concentration waves are rapidly amplified; long wavelengths giving rise to clustering (spinodal decomposition) and short wavelengths giving rise to continuous ordering. As the amplitude of the concentration waves increases the anharmonic terms in the free energy expansion become important and the harmonic waves are distorted or modulated by the emergence and preferred growth of higher-order waves generally producing peaks at other superlattice locations. It is important to note that continuous transformation in both clustering and ordering involving first-order transitions is akin to a second-order transition except that continuous transformation in the former case occurs under conditions generally far removed from equilibrium, whereas in second-order transitions the homogeneous order-disorder reaction can occur under equilibrium conditions. See Figure 1.

Early Works of the "Spinodal Era"

The notion of a "wave-like" clustering or periodic redistribution of solute during aging was first suggested by Daniel and Lipson (22) to explain the appearance of "sidebands" or "satellites" in X-ray studies of precipitation in Cu-Ni-Fe alloys. The development of the concept of spinodal decomposition in the theoretical works of Hillert (11,12) and Cahn (3,4,13) provided a fundamental basis for the evolution of quasi-periodic composition modulations or concentration waves during the decomposition of supersaturated solid solutions. This new model of precipitation proved to be useful as a tool for interpreting consistently a variety of experimental observations in a number of alloy systems and has been comprehensively and critically reviewed (23,24,25). Eventually the construct of concentration waves proved to be useful also for describing continuous ordering reactions in the short

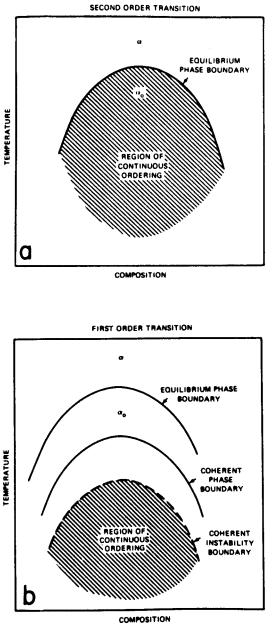

Fig. 1. (a) Region of continuous ordering relative to the equilibrium phase boundary for a second order transition, (b) region of continuous ordering shown schematically relative to the equilibrium and coherent phase boundaries for a first order transition.(21)

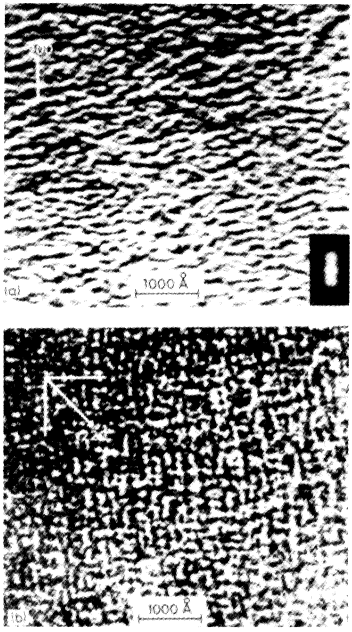

Fig. 2. Triaxially modulated structure developed in a Cu-31.6 Ni-1.7 Cr alloy aged at 650°C for 1 hr revealed by matrix strain contrast striations along the traces of {100} planes (a) $\vec{g}=\bar{2}00$ (b) $\vec{g}=220$; foil normal near [001].(37)

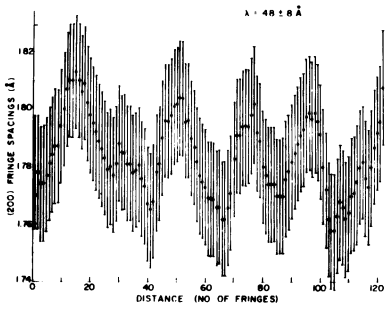

Fig. 3. Periodic variation of lattice fringe spacing in the lattice image of a spinodally decomposed Cu-28.9 Ni-2.8 Cr alloy aged at 700°C for 10 minutes. (38)

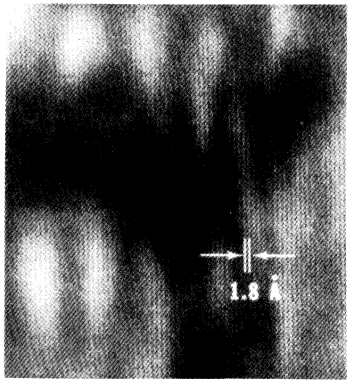

Fig. 4. Lattice image of (200) planes in spinodally decomposed Au-77 a/o Ni alloy. (39)

wavelength regime (14,15) as described above.

Preliminary electron microscopy observations appeared which revealed periodic arrays of particles or periodic contrast striations accompanying the so-called "sideband" effects, and these "modulated structures" were interpreted in terms of a spinodal reaction. Ardell and Nicholson (26), however, in an important study of aged Ni-Aℓ alloys, recognized that aligned arrays of γ' particles could evolve during stress-affected coarsening of an initially random distribution of particles and, thus, not necessarily stem from spinodal decomposition. During this active period some electron microscopy work on the classic Cu-Ni-Fe alloy appeared (27), but it was Thomas and co-workers at Berkeley that published the definitive electron metallographic study of spinodal decomposition in Cu-Ni-Fe alloys (28). Above all, the Berkeley work revealed that periodic and aligned microstructures formed during the earliest stages of decomposition in these pseudo-binary, "sideband alloys," and that the general behavior was consistent with the basic tenets of the spinodal theory. Butler and Thomas (28) showed the characteristic quasi-periodic strain contrast images associated with compositional modulations along the ⟨100⟩ matrix directions. The periodic and aligned, two-phase mixtures which develop after prolonged aging were documented systematically as well. In many ways this work set a model or standard for numerous subsequent studies as this mode of phase transformation and its different variations were recognized and studied in other binary and ternary systems.

Survey and Analysis of Experimental Results

Cu-Ni-Cr and Au-Ni: Phase Separation (FCC)

The ternary Cu-Ni-Cr alloys were reported to be "sideband alloys" similar to Cu-Ni-Fe as early as 1958 by Manenc (29). Badia et al. (30,31) verified the occurrence of sideband phenomena and the formation of the so-called modulated structures during aging within the ternary miscibility gap and concluded that spinodal decomposition occurred in these Cr-hardened cupronickels. Kreye and Pech (32) in a limited electron microscopy study also rationalized their results in terms of a spinodal reaction. During this period Morral and Cahn (33,34) and de Fontaine (35) extended the treatments of spinodal decomposition in binary systems to consider diffusional instabilities in ternary systems. Wu and Thomas (36) and Chou et al. (37) later comprehensively investigated the decomposition process and the resultant microstructural development. Wu, Sinclair, and Thomas (38) applied the lattice imaging technique and optical microanalysis to characterize the modulated structures or "wave-like" composition variations occurring during the early stages of decomposition. This approach provides an estimate of both the amplitude and wavelength of the compositional modulations. Electron micrographs of a Cu-31.6 Ni-1.7 Cr alloy aged at 650°C for 1 hour, shown in Fig. 2, clearly reveal the development of a triaxially modulated structure resulting from the formation of concentration waves along the ⟨100⟩ matrix directions. The attendant variations in the lattice parameter giving rise to the strain contrast striations are revealed clearly in the variation of the lattice fringe spacing in an aged Cu-28.9 Ni-2.8 Cr alloy exhibiting a similar modulated structure as shown in Fig. 3.

Sinclair, Gronsky and Thomas (39) also applied lattice imaging electron microscopy to characterize the wavelength and amplitude of the composition variations in the binary Au-Ni alloys. Fig. 4 shows a typical lattice image of the modulated structure and Fig. 5 displays the variation of the d-spacing. It should be noted that a coarse background intensity variation is superimposed on the lattice fringe image and that this large scale intensity

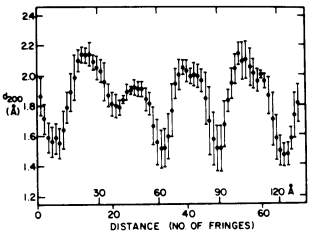

Fig. 5. Variation of the fringe spacing versus distance in the lattice image of the Au-Ni alloy. (39)

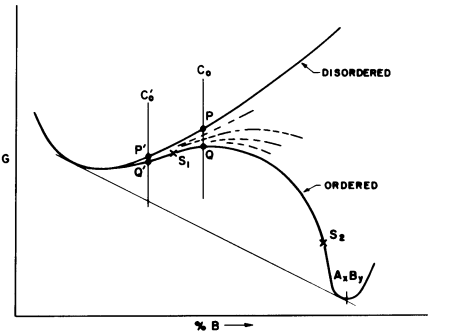

6(a)

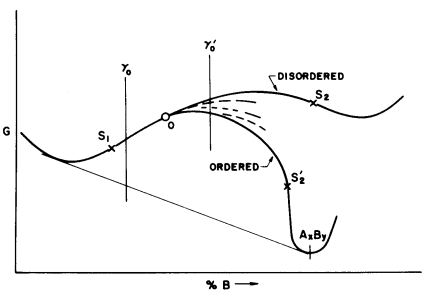

6(b)

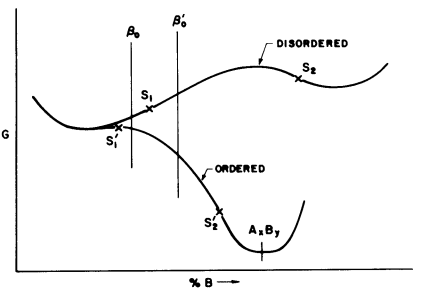

6(c)

Fig. 6. Hypothetical free energy-composition diagrams for homogeneous disordered and ordered solid solutions.

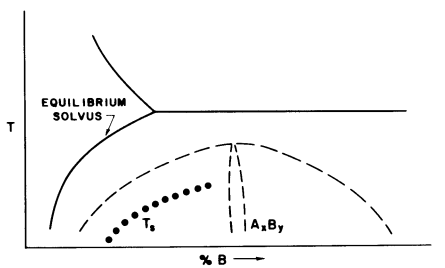

Fig. 7. Hypothetical phase diagram depicting metastable A_xB_y phase.

variation directly reflects the modulated structure; the wavelength of these intensity variations is about 29Å and this agrees well with that determined from the sidebands or satellites in the electron diffraction pattern. Lattice imaging is a potentially powerful tool for quantitatively characterizing the long range compositional fluctuations which develop in spinodally decomposing (and ordering) alloys; however, some questions still exist concerning the correlations between the magnitude of the fringe spacings and the actual three-dimensional structures which produce the lattice image as pointed out by other investigators (40). For example, in this Au-Ni work apparent lattice spacings in Ni-rich and Ni-poor regions greater than the spacings of pure Ni and pure Au, respectively, are measured. (See note added in proof.)

Phase Separation and Ordering in FCC Solid Solutions: Ni-Ti, Co-Ti, Co-Fe-Ti and Ni-Aℓ

Precipitation in Ni-Ti alloys containing about 10-15 a/o Ti has been studied by a number of investigators using X-ray diffraction (41-43), electron microscopy (44), field ion microscopy (FIM), (45) and atom probe techniques (APFIM), (9) and various physical property measurements (46). At large undercoolings the supersaturated solid solutions decompose producing a metastable, coherent ordered Ni_3Ti (γ') phase having the $L1_2$ superstructure. The equilibrium precipitate is an ordered hexagonal η phase with the Ni_3Ti stoichiometry. Based on the early metallographic studies of Manenc and coworkers (41-43) and their own magnetic measurements, Ben-Israel and Fine (46) as early as 1963 concluded that spinodal precipitation occurs in this system giving rise to a periodic array of γ', Ni_3Ti particles. The electron microscopy study of Saito and Watanabe (44) of a Ni-12 a/o Ti alloy clearly revealed the formation of fine, periodic contrast striations with a spacing of about 100Å along the traces of the {100} matrix planes during the early stages of decomposition and concomitant appearance of diffuse "satellites." They also showed that weak $L1_2$ (γ') superlattice reflections appear very early in the precipitation reaction. Similar results were obtained by Laughlin (8) in a systematic study of the early stages of decomposition of Ni-10 a/o and 12 a/o Ti alloys. Periodic arrays of coherent cuboidal particles developed at maximum hardness as shown by Saito and Watanabe (44). Sass and Cohen (47) also revealed the periodic and aligned γ' particles in an early electron microscopy study. Sinclair, Ralph, and Leake (45) reported an interesting application of FIM to the study of precipitation in the Ni-Ti system. By carefully following the field evaporation behavior of a Ni-14 a/o Ti alloy these workers concluded that the ordered γ' precipitates evolve continuously via a spinodal mechanism involving clustering and ordering and that the early stages of decomposition are characterized by a diffuse interface between the disordered and ordered regions. The mechanism suggested in their work involves virtually a simultaneous or cooperative clustering and ordering, that is, the increase in order parameter occurs in parallel with the increase in local Ti concentration. The notion that the formation of the γ' phase occurs via a homogenous or continuous transformation involving a process of clustering and ordering has been emphasized in the more recent electron microscopy work of Laughlin (8). Laughlin suggested that the Ni-Ti solutions decompose via a spinodal mechanism producing Ti-enriched and Ti-depleted regions and after some critical Ti concentration is exceeded the Ti-enriched regions order continuously to the $L1_2$ superstructure.

The systematics of possible reaction paths involving clustering and ordering in the Ni-Ti system can be elucidated using a simple approach based on graphical thermodynamics or free energy-composition curves. This approach will be useful for analyzing a number of other systems as well. In Fig. 6

a series of hypothetical free energy-composition diagrams are shown consistent with the metastable phase reaction depicted in Fig. 7. The free energy curve associated with the disordered solid solution is considered concave upwards at all compositions in Fig. 6a. The ordered free energy curve represents the free energy of a homogeneous ordered phase of optimum order parameter. Clearly, the free energy curve for the ordered solution is a projection of a locus along the G-c-η surface, η being the order parameter. One can imagine a hierarchy of free energy curves ranging from SRO to imperfect LRO between the disordered and lowest ordered curve. For this free energy-composition scheme, spinodal decomposition can only occur if the supersaturated solid solution orders first. A disordered solid solution of composition C_o is metastable with respect to precipitation of the A_xB_y (Ni_3Ti) phase; however, the solution can lower its free energy from P to Q by ordering. This partially ordered state is unstable with respect to phase separation and the system can undergo a spinodal reaction involving continuous clustering and ordering leading to a metastable two-phase mixture. Here the spinodal reaction is entirely contingent on prior ordering and is termed a conditional spinodal after Allen and Cahn (48). On the other hand, the composition C_o' which is also metastable with respect to precipitation of the ordered phase, can lower its free energy from P' to Q' by ordering. This ordered state is, of course, still metastable with respect to the formation of the A_xB_y phase.

The clustering and ordering processes may also be interpreted in terms of the slightly modified schemes shown in Figs. 6b and 6c. Here the disordered free energy curve also shows inflections and phase separation. Some different reaction paths become evident. In Fig. 6b a disordered solid solution of composition γ_o is unstable with respect to phase separation and spontaneous unmixing will occur leading to solute-enriched and solute-depleted regions. When the composition in the solute-enriched region exceeds the composition O, this region will order. A continuous phase separation involving clustering and ordering can then proceed, eventually generating the two-phase mixture denoted by the common tangent construction. In this case, clustering precedes the ordering reaction and then the system progresses toward equilibrium via cooperative clustering and ordering (6-8). The composition γ_o' is unstable with respect to clustering and ordering, i.e., long wavelength and short wavelength fluctuations. It is likely that short range atomic exchanges occur rapidly to produce ordering, relaxing the free energy along the G-c-η surface toward the ordered curve. Simultaneously a spinodal reaction leading to continuous unmixing or phase separation can occur. This is in contrast to the previous case (γ_o) in which the supersaturated state is unstable initially only with respect to long wavelength compositional fluctuations. The supersaturated state β_o (Fig. 6c) is analogous to C_o in Fig. 6a; a conditional spinodal reaction can occur following ordering. β_o' in Fig. 6c is essentially the same as γ_o' in Fig. 6b.

The possible synergistics of clustering and ordering are rather apparent from the discussion above. The reaction paths suggested by Sinclair, Ralph, and Leake (45) and Laughlin (8) are essentially described by the states γ_o' and γ_o, respectively. Watts and Ralph (9) in a study of the early stages and transformation in a Ni-12 a/o Ti alloy using APFIM and TEM suggested that ordering may precede phase separation. However, the argument presented by them is a bit ambiguous and although such a reaction path is possible their evidence is unconvincing (10).

Similar precipitation processes have been observed and studied in Co-Ti (49) alloys and in the ternary cobalt-rich Co-Fe-Ti (50,51) alloys. In Fig. 8a the lineal contrast striations characteristic of the "sideband" state are shown, and in Fig. 8b, the periodic, coherent two-phase mixture or

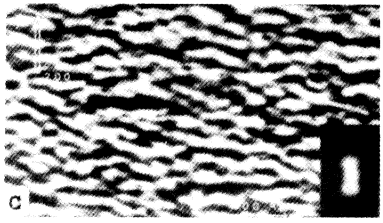

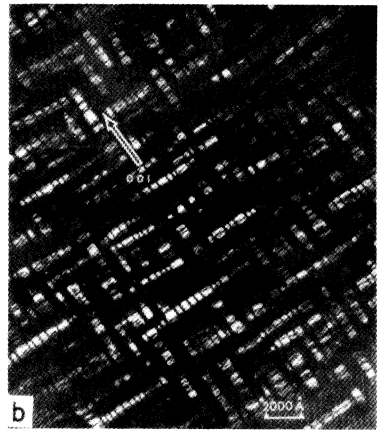

Fig. 8. (a) Strain contrast striations along the traces of the {100} matrix planes in a spinodally decomposing Co-Fe-Ti alloy; insert shows the satellite flanking the 200 reflection, (b) periodic array of γ' particles resulting from precipitation in a Co-Fe-Ti alloy. (50)

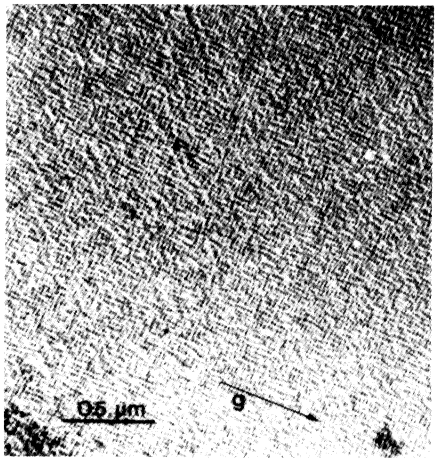

Fig. 9. "Spinodal microstructure" developed in a Cu-5^{w}/o Ti alloy aged 100 minutes at 450°C.(6)

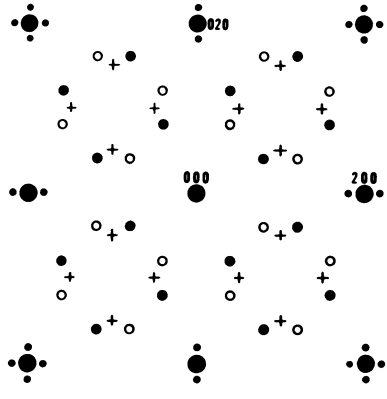

Fig. 10. Schematic of an (002) diffraction pattern of an as-quenched Cu-Ti alloy showing the positions of the $\{1\frac{1}{2}0\}$ diffuse scattering (+), $D1_a$ superlattice reflections (0,●) and satellite spots.(6)

modulated structure which evolves is revealed in dark-field using an $L1_2$ superlattice reflection. The reaction path in these systems also appears to involve essentially a concomitant clustering and ordering. Hill and Ralph (52) used APFIM to study the early stages of transformation in a Ni-14 a/o Aℓ alloy and concluded that the alloy initially decomposes by a spinodal mechanism at large undercoolings. They arrived at this result based on a Fourier analysis of atom probe composition profiles. However, the composition profiles suggest that discrete γ' particles had already evolved and thus the results are somewhat questionable.

Cu-Ti and Cu-Ni-Sn: Complex Clustering and Ordering (FCC)

Precipitation in the Cu-Ti system also illustrates quite nicely the interplay of clustering and ordering processes. A number of investigators have studied the precipitation process using a variety of experimental techniques (6,7,53-59). The recent electron microscopy results have been particularly fruitful in elucidating the nature of the reaction sequence involving clustering and ordering and the formation of the metastable $D1_a$ (Cu_4Ti) phase. The "spinodal microstructure" is shown in Fig. 9. The system may be particularly unique exhibiting both "spinodal ordering" (ordering instability) and spinodal phase separation involving concomitant clustering and ordering including a conditional spinodal. The ordering instability is essentially similar to that occurring in the Ni-Mo system deriving from "special point" positions in the first Brillouin zone, viz. $\{1\frac{1}{2}0\}$. The development of the $\frac{1}{4}\langle 420\rangle$ waves relaxes the free energy from the homogeneous disordered state along the G-c-η surface towards the ordered curve. The anharmonic terms in the free energy effect of the emergence of the $\frac{1}{5}\langle 420\rangle$ concentration waves which generate the imperfectly ordered $D1_a$ structure. The reaction path, thus, can then be imagined to involve spinodal ordering, taking the system from P towards Q in Fig. 6a, leading to subsequent instability with respect to phase separation as discussed above. Hakkarainen (54), and Laughlin and Cahn (6) have reported the appearance of $\{1\frac{1}{2}0\}$ diffuse scattering during the early stages of decomposition. However, it is extremely difficult to distinguish experimentally this reaction path categorically from others described earlier (e.g. γ_o). This is because the various scattering effects ($\{1\frac{1}{2}0\}$ diffuse scattering, satellites, $D1_a$ reflections) are extremely weak and simultaneously present from the very earliest stages observed in the decomposition process. (See Fig. 10.)

Biehl and Wagner (59) have studied the decomposition of supersaturated Cu-Ti solid solutions using APFIM. The composition profiles (Ti-concentration versus distance) were determined by successive field evaporations over distances of about 400-500 atomic layers close to a $\langle 111\rangle$ direction. The concentration profile for a Cu-2.7 a/o Ti specimen aged for 10 minutes at 623 K indicates that the composition modulations during the very early stages of decomposition generally exhibit extrema below the Cu_4Ti composition. After aging 500 minutes at 623 K the extrema in the concentration profiles appear to reach the composition of the Cu_4Ti phase. This progressive build-up of the amplitude of the Ti-enriched regions is certainly consistent with the notion of continuous phase separation and ordering occurring in this system. Fourier transformations of the concentration profiles revealed a Fourier spectrum consisting of a range of wavelengths during the early stages of decomposition with the distribution becoming sharper with prolonged aging. This APFIM study never detected an early stage where the wavelength of the composition fluctuations remained constant while the amplitude increased continuously as reported previously (6). Generally, between 10 and 500 minutes at 623 K the average wavelength and amplitude progressively increase.

In Fig. 11, the details of the satellite positions in reciprocal space

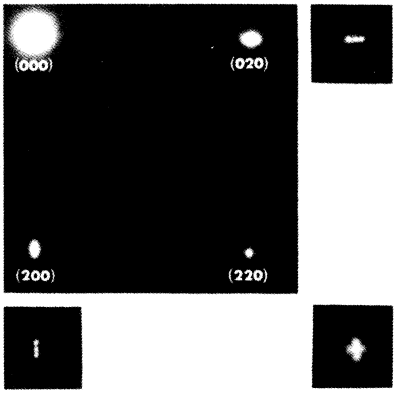

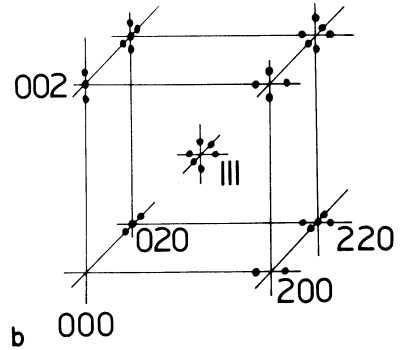

Fig. 11. (a) (002) electron diffraction pattern from a spinodally decomposed Cu-Ti alloy showing the satellite configuration flanking the matrix reflections, (b) schematic showing disposition of satellites in reciprocal space predicted for a triaxially modulated structure, (c) sideband behavior at a (200) reflection in a Cu-2.9^{a}/o Ti alloy during aging. (7,54)

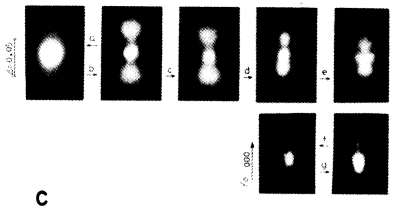

Fig. 12. Sidebands in the X-ray diffraction pattern from a Cu-4^{w}/o Ti alloy clearly showing symmetrical satellites during the early stages of decomposition and the development of asymmetry in position and intensity after prolonged aging. (60)

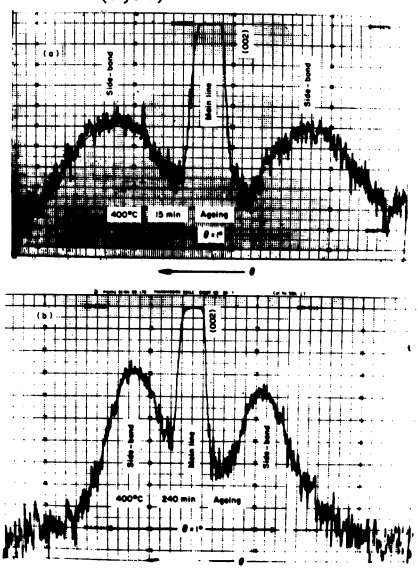

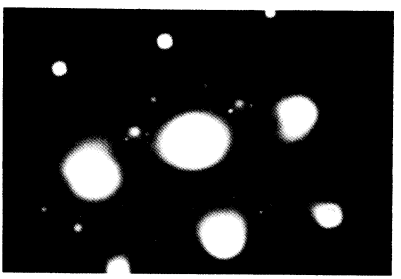

Fig. 13. The [001] pattern of a Ni-16.7^{a}/o Mo alloy aged at 750°C for 20 min. Sharp LRO reflections are observed at $\frac{1}{5}$ {420}.

are shown. The evolution of the asymmetry in the position of satellites is also documented by electron diffraction (54). Fig. 12, from the work of Tsujimoto, Hashimoto and Saito (60) illustrates the asymmetry in intensity as well as position in the evolving sidebands of an X-ray diffraction pattern of Cu-Ti. Note that the sidebands are fairly symmetric after 15 min. aging at 400°C, but after 240 min. the high-angle sideband is more intense and closer to the fundamental reflection.

Since the work of Daniel and Lipson (22), numerous models have been proposed to explain the behavior of sidebands during aging (60-66). Recently, Tsujimoto et al. (60) proposed a model which considers scattering by an "imperfect macrolattice" of "unit regions." The model seems to account reasonably well for a number of features such as the asymmetries of position and intensities as well as the movements of the sidebands observed during aging in the Cu-4 w/o Ti and Ni-10 w/o Ti spinodal alloys. Hakkarainen has proposed a similar model (54).

The recently developed commercial age hardening Cu-Ni-Sn alloys (Cu-15 w/o Ni-8 w/o Sn, Cu-10 w/o Ni-6 w/o Sn) have been shown to decompose spinodally exhibiting modulated structures and associated diffuse scattering effects (67). The phase separation is accompanied by DO_{22} ordering within the Sn-enriched phase (68,69). A great deal of effort has been directed towards evaluating the strengthening deriving from the spinodal process in these alloys (67,70). Ditchek and Schwartz (69) have reported an interesting X-ray diffraction study of the behavior of the sidebands in this system in terms of a nonlinear theory of spinodal decomposition recently developed by Tsakalakos and Hilliard (71).

Spinodal and Continuous Ordering: Ni-Mo and Cu_3Au

Alloys of Ni-Mo have been investigated over the range of 10 a/o Mo to 25 a/o Mo by various investigators. Among the phases which form are the $D1_a$, DO_{22} and Pt_2Mo, though only the $D1_a$ phase is an equilibrium one. These superstructures correspond to the stoichiometry Ni_4Mo, Ni_3Mo and Ni_2Mo, respectively. Each of these structures are crystallographic derivatives of the A1 (fcc) structure, and are composed of ordered layers of {420} planes (72,73). For example, the Ni_4Mo structure has one Mo {420}, followed by four Ni {420} planes, followed by one Mo {420} and so forth. We shall focus on the formation of the $D1_a$ phase.

Alloys in the range of 14 a/o Mo to 20 a/o Mo that are solution treated in the single phase region all contain diffuse scattering at the $\{1\frac{1}{2}0\}$ positions in reciprocal space after quenching to room temperature. D. de Fontaine has presented a model which describes the local order of such an alloy in terms of $\{1\frac{1}{2}0\}$ ordering modulations (5,73). It has been observed that the intensity at the $\{1\frac{1}{2}0\}$ reflections increases with time, when the alloy is held below the equilibrium solvus. This buildup of the $\{1\frac{1}{2}0\}$ ordering wave corresponds to a decrease in the free energy of the alloy. However, in this composition range, the formation of the equilibrium $D1_a$ phase (Ni_4Mo) is favored, thus the initial increase in $\{1\frac{1}{2}0\}$ ordering is expected to be followed by the formation of the Ni_4Mo phase.

Two distinct mechanisms have been observed for this process. At higher temperatures ($T > 750°C$ for Ni 16.7 a/o Mo; $T > 800°C$ for 20 a/o Mo) the equilibrium $D1_a$ phase forms by the nucleation of highly ordered particles in a matrix of SRO (74,75). This corresponds to a lowering of the free energy from Q' to the common tangent in Fig. 6a. The electron diffraction pattern of an alloy that has undergone such a process is shown in Fig. 13. Note that the $D1_a$ reflections are quite sharp and appear in conjunction

with the $\{1\frac{1}{2}0\}$ reflections (cf. Fig. 10). This process also occurs in the stoichiometric alloy, except in this case the matrix eventually transforms completely to the ordered phase. Further aging eventually depletes the $\{1\frac{1}{2}0\}$ position of intensity, and the diffraction of the off-stoichiometric alloy pattern looks as shown in Fig. 14.

At larger undercoolings, the $\langle 1\frac{1}{2}0\rangle$ ordering waves begin to grow without bound, i.e., become unstable. The linearized kinetic model developed by de Fontaine (5) no longer is valid, and the anharmonic terms of the free energy expression must be included. This in turn leads to a continuous change in the local order, changing from ordering waves of $\frac{1}{4}\langle 420\rangle$ to $\frac{1}{5}\langle 420\rangle$. This continuous change in wavelength of the ordering modulations evidences itself in electron diffraction as a continuous transfer of scattered intensity from the $\{1\frac{1}{2}0\}$ positions to the $\frac{1}{5}\{420\}$ positions (viz. those of the equilibrium $D1_a$ phase). See Fig. 15. Note that the diffuse intensity streaks are located solely between the $\{1\frac{1}{2}0\}$ and $\frac{1}{5}\{420\}$ positions. Their absence on the low-angle side of the $\frac{1}{5}\{420\}$ demonstrates that the intensity streaks are not due to a shape effect. The process has been termed "spinodal ordering" by de Fontaine, since the initial instability is not of the equilibrium ordering wave ($\frac{1}{5}\langle 420\rangle$), but of the "special point" $\langle 1\frac{1}{2}0\rangle$ ordering wave. At large enough undercoolings the solid solution also should become unstable with respect to $\frac{1}{5}\langle 420\rangle$ waves, but the $\langle 1\frac{1}{2}0\rangle$ will most probably dominate initially (73). Hence, for large enough undercoolings in Ni-Mo, we have an example of a continuous ordering process without concomitant phase separation by spinodal decomposition. (cf. Fig. 1b).

Chen and Cohen (76) have used X-ray diffuse scattering to determine the temperatures for continuous ordering or ordering instability below T_c for several binary alloys. The intensity at some position $\vec{k}$ in reciprocal space due to short range order or a composition wave of wave vector $\vec{k}$ is proportional to the square of the amplitude of this Fourier component and is given by Equation (3) above. This intensity diverges at the superlattice position $\vec{k}^*$ at the instability temperature T_i. Rewriting Equation (3) in the form

$$I_{SRO}(\vec{k}) = \frac{k_B T}{k_B(T-T_i) + J(\vec{k}) - J(\vec{k}^*)}$$

where the parameter $J(\vec{k})$ is proportional to the Fourier transform of the interaction potential, and $k_B T_i + J(\vec{k}^*) = 0$, it is apparent that the function $T/I_{SRO}(\vec{k}^*)$ should be linear with temperature and extrapolate to zero at the instability temperature, T_i. This was proposed in the review by Cook (21). In Fig. 16, the term $T/I_{SRO}(\vec{k}^*)$ is plotted against T for Cu_3Au. A temperature of 358.2°C is predicted for the onset of continuous ordering compared to T_c = 382.2°C

Continuous Phase Separation in BCC Solid Solutions (Nb-Zr, Fe-Mo, Fe-Cr, and Fe-Cr-Co Alloys)

Flewitt (77) has observed the formation of modulated structures in Nb-rich Nb-Zr alloys during aging above and below the monotectoid temperature in the system. The compositional modulations develop along the {100} planes and an array of satellites appear in the diffraction patterns flanking the matrix reflections as expected for a triaxially modulated structure. The elastic anisotropy factor $2C_{44}/C_{11}-C_{12}$ for pure Nb is less than unity, suggesting the possibility of $\langle 111\rangle$ compositional waves. However, in these concentrated alloys (~20-40 a/o Zr) the Zr markedly changes the anisotropy factor and the data indicate that the elastic anisotropy is likely to become greater than one in the alloys consistent with the observations of $\langle 100\rangle$ modulations (78). The calculated spinodal regime and estimated coherent

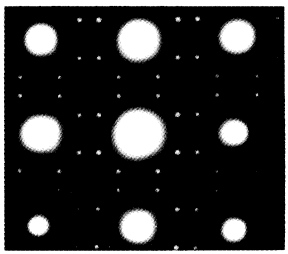

Fig. 14. Ni-16.7[a]/o Mo aged at 700°C for 10,000 min. [001] zone axis (74).

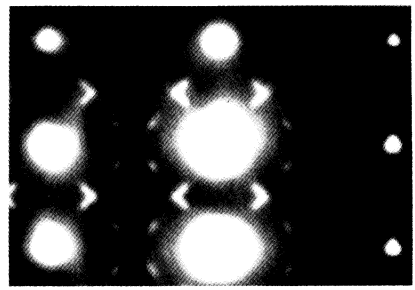

Fig. 15. Ni_4Mo alloy aged 10 min. at 650°C. Note the continuous intensity distribution from the $\{1\frac{1}{2}0\}$'s to the $D1_a$ superlattice positions (72).

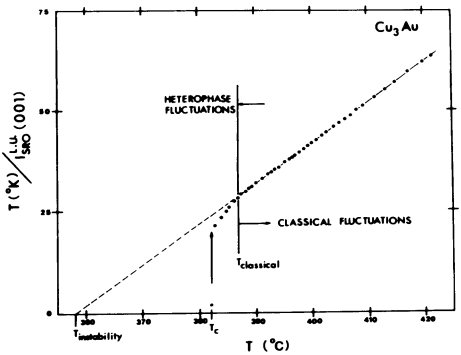

Fig. 16. Plot of $T(K)/I_{SRO}$ at the (001) position versus T(K) for Cu_3Au (76).

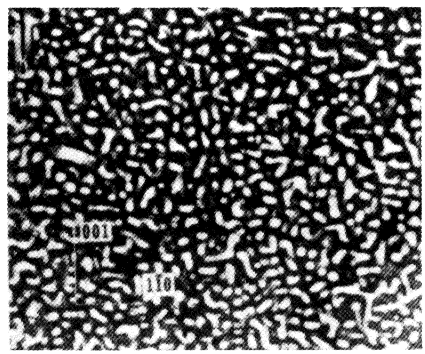

Fig. 17. Isotropic "spinodal microstructure" in an Fe-31[w]/o Cr-23[w]/o Co alloy aged for one hr at 660°C (92).

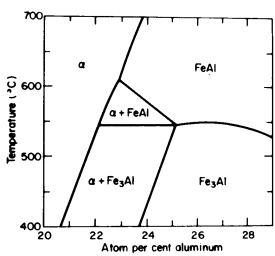

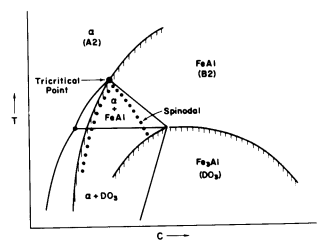

Fig. 18. (a) The modified coherent Fe-Aℓ phase diagram (48), (b) schematic Fe-Aℓ coherent phase diagram showing higher-order transition lines, and the tricritical point.

spinodal agree rather well in this system. Below the monotectoid temperature the spinodal reaction involves a metastable homogeneous phase separation into two coherent bcc phases (Zr-enriched and Zr-depleted) and during prolonged aging the modulated structures transform to produce discrete plates or discs along the {100} planes having an h.c.p. structure.

The precipitation processes occurring in Fe-Mo bcc solid solutions have been studied extensively over the years (79-81). Miyazaki et al. have recently shown the occurrence of a metastable spinodal reaction in concentrated alloys containing 17-20 a/o Mo. This continuous decomposition is suggested to be associated with a metastable miscibility gap spanning the Fe-Mo phase diagram.

The decomposition of Fe-Cr (and Fe-Cr-X) alloys at low temperatures has been of interest for over thirty years because of the role of this process in the embrittlement of commercial alloys (82-86). It is generally recognized that the fine-scale precipitation involves the formation of a Cr-rich ferritic phase (α') within the miscibility gap intersecting the σ phase region in the phase diagram. It has been proposed that α' forms by spinodal decomposition (87,88); however, conventional electron microscopy and X-ray diffraction studies have been of limited success in characterizing the decomposition because of the small strain effects accompanying the reaction and because of the small difference in scattering factors between Fe and Cr. Brenner, Miller and Soffa (84) recently have studied the decomposition of an Fe-32 a/o Cr alloy aged at 470°C within the miscibility gap using atom probe field ion microscopy (APFIM). The preliminary atom probe data show that the decomposition is occurring via continuous phase separation whereby the composition of the Cr-rich regions is amplified progressively. The maximum composition within the Cr-rich regions after long aging times ($\sim$200 hours) is still well below the equilibrium composition. Furthermore, the morphology of the decomposition product appears to be an interwoven network of interconnected "veins" expected for spinodal structures in systems where the influence of elastic anistropy is small (90). This is consistent with the fact that the strain in the system is small.

The Fe-Cr-Co ternary permanent magnet alloys which have been developed over the past several years exploit the spinodal reaction occurring in the Fe-Cr system to produce a fine-scale structure consisting of an Fe-rich phase (α_1) and a chromium-rich phase (α_2) (91). Cobalt raises and widens the miscibility gap and thus provides enhanced precipitation kinetics (92). Spinodal decomposition in these ternary alloys also appears to be essentially isotropic as shown in Fig. 17.

Clustering and Ordering in BCC Solid Solutions: Fe-Aℓ, Cu-Mn-Aℓ, Fe-Be and Cu-Zn

An important paper on continuous transformations is the work of Allen and Cahn (48) which appeared in 1976. In this investigation of the mechanisms of phase transformations occurring in Fe-rich Fe-Aℓ alloys, the different modes of ordering and phase separation are discussed in terms of the coherent phase diagram shown in Fig. 18. An important feature of the approach is that the mechanisms of transformation for various undercoolings or supersaturations are deduced and categorized directly in terms of the thermodynamic schemes which are consistent with the phase diagram and from simple kinetic principles, e.g., because of the relative diffusion distances involved, continuous ordering transitions occur more rapidly than phase separation within a miscibility gap once the ordering lines have been crossed. The necessary free energy relationships give rise to limits of stability with respect to continuous ordering and phase separation, and various

reaction sequences involving ordering and spinodal decomposition are predicted. The thermodynamic analysis of the Fe-Aℓ system suggests that the system exhibits a tricritical point (93), where an order-disorder reaction (higher-order, λ transition) uniquely intersects a miscibility gap. Furthermore, the notion of a conditional spinodal contingent on prior ordering, as discussed above, is introduced. Allen and Cahn (48) also discuss the perturbation of the transformation modes as a result of APB's produced in the B2 and DO_3 superstructures. This work emphasizes well the notion that phase separation and ordering are not mutually exclusive phenomena but can occur in the same system, often in a cooperative or interdependent manner.

Spinodal decomposition within an ordered phase is illustrated in Fig. 19. The Fe-24 Aℓ alloy was treated first at 625°C to produce a single phase Fe-Aℓ (B2) structure characterized by large B2 domains. The large domain structure minimizes the influence of the APB's on the subsequent transformation of the B2 phase and allows homogeneous transformations to be observed. In Fig. 19, phase separation or continuous decomposition is revealed within the B2 phase after aging at 570°C. The spinodal morphology is like that of spinodal decomposition in an isotropic system or where the elastic contribution to the free energy is small, as discussed earlier. Here a conditional spinodal reaction requiring first B2 ordering separates the initially homogeneous Fe-Aℓ phase into a disordered α-phase and an ordered phase (B2) of different compositions. The micrographs in Fig. 20 clearly indicate an alternate reaction path at 539°C involving a spinodal reaction in the B2 phase and subsequent DO_3 ordering. The initial Fe-Aℓ phase (B2) separates into Aℓ-enriched and Aℓ-depleted regions and the Aℓ-enriched regions then undergo continuous ordering. In all the micrographs the antiphase boundary structure in the Fe-Aℓ phase is outlined by a continuous layer of disordered α-phase which "wets" the boundaries.

The pairwise interaction or interchange energies for both first and second neighbor interactions are negative in the Fe-Aℓ system; that is, A-B pairings are favored in the first and second neighbor shells. Thus, the B2 and DO_3 structures are expected at different temperatures for certain concentration ranges (94,95). Hasaka (96) using the method of Ino (97) has analyzed the composition and temperature dependence of the free energies of the B2, DO_3 and disordered α phases using a pairwise interaction model including 3rd nearest-neighbors. The ordering and phase separation processes can be understood in Fe-Aℓ alloys in terms of the tendency for pairs of unlike atoms between first and second nearest-neighbor sites and like atoms between third neighbor sites. The equilibrium phase diagram obtained is essentially in accord with that of Allen and Cahn but includes a DO_3 + B2 two-phase region.

Bouchard and Thomas (98) have studied an interesting conditional spinodal reaction in the $(Cu\text{-}Mn)_3$ Aℓ ternary alloys. The alloys investigated in this work lie along the $Cu_3Aℓ$-$Cu_2MnAℓ$ composition line and can be designated $Cu_{3-x}Mn_xAℓ$ with $0 < x < 1$.[3] The binary $Cu_3Aℓ$ phase exhibits the DO_3 structure at low temperatures and undergoes a $DO_3 \rightarrow B2$ transition at intermediate temperatures. The ternary $Cu_2MnAℓ$ phase is the well-known Heusler alloy having the $L2_1$ structure at low temperatures and undergoes a $L2_1 \rightarrow B2$ reaction at intermediate temperatures. At higher temperatures both phases have a disordered bcc structure (β). The DO_3 and $L2_1$ superstructures are closely related and form a continuous series of ordered solid solutions (DO_3-$L2_1$) at lower temperatures. At even lower temperatures, a miscibility gap appears in the DO_3-$L2_1$ phase field leading to decomposition of the single phase ordered solid solution into a two-phase mixture of $Cu_3Aℓ$-rich DO_3 regions and $Cu_2MnAℓ$-rich $L2_1$ regions. The phase separation occurs by rearrangement of Cu and Mn atoms on one of the sub-lattices of the structure. A schematic of the structures and

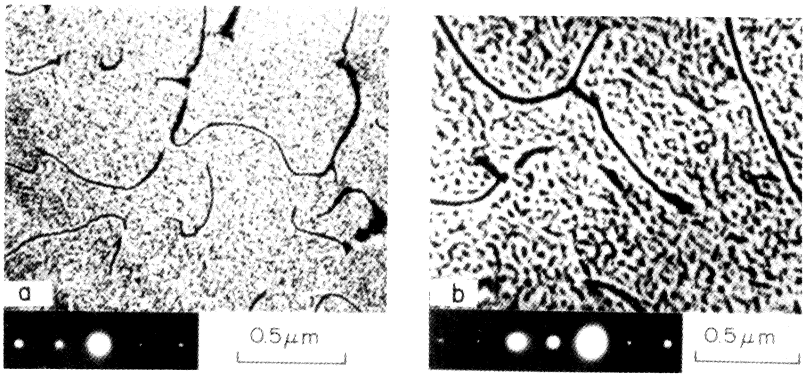

Fig. 19. Spinodal decomposition within the ordered FeAℓ (B2) phase in an Fe-24% Aℓ alloy decomposed at 570°C for (a) 1 min., (b) 5 min. prior to quenching. These dark-field micrographs were imaged using a FeAℓ (B2) superlattice reflection (48).

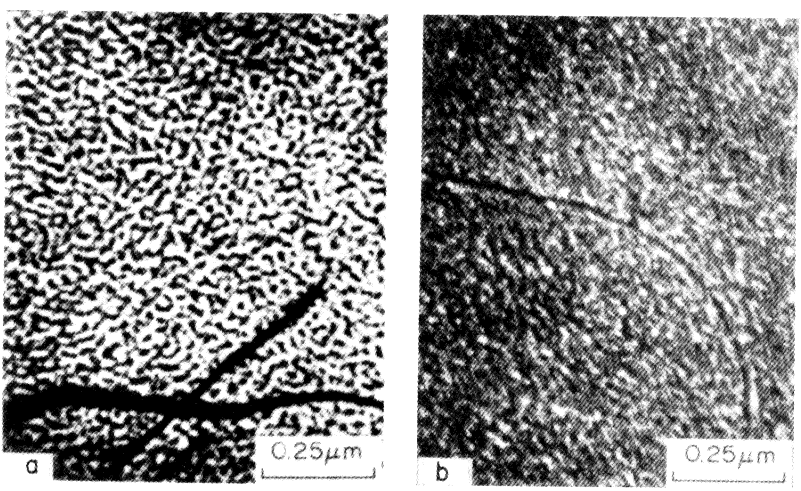

Fig. 20. Spinodal decomposition in the FeAℓ (B2) ordered phase followed by continuous ordering (DO_3) in the Aℓ-rich regions during aging at 539°C; (a) (222) dark-field showing continuous decomposition of B2, (b) (111) dark-field revealing a high density of fine domains of the DO_3 phase in the Aℓ-rich regions (48). (Note: indexed according to the DO_3 unit cell. See Ref. 48.)

a phase diagram are depicted in Fig. 21.

A symmetrical alloy (x = 0.5) cooled from the β phase region will first undergo an A2-B2 ordering reaction, the Cu atoms preferentially occupy two of the four interpenetrating fcc sublattices and the other Cu, Aℓ, and Mn atoms are distributed over the other two. On further cooling a third sublattice is occupied by Aℓ at the $B2 \rightarrow (DO_3\text{-}L2_1)$ transition with the remaining Cu and Mn atoms randomly mixed on the fourth. At still lower temperatures unmixing occurs on the fourth sublattice within the miscibility gap as mentioned above. Well within the gap the phase separation is observed to occur via a continuous decomposition of the ordered phase. A modulated structure and satellites are observed resulting from the development of compositional waves within the fourth sublattice along the ⟨100⟩ matrix direction as shown in Fig. 22. The spinodal reaction is also observed in the asymmetrical alloy x = 0.8. In this system the conditional spinodal reaction separates an ordered phase into two related ordered phases of differing compositions.

In Fe-Be alloys the continuous reactions involving clustering and ordering reported by various investigators (99,100) can be understood in terms of pairwise interactions between first and second neighbor atoms as shown by Richards (94) and Ino (97). The models assume that the interchange energies favor unlike nearest neighbor pairs and like pairs of atoms for the second neighbors.

Higgins, Nicholson and Wilkes (100) recognized the occurrence of a spinodal reaction in this system but did not provide a systematic thermodynamic basis for the reaction paths. An Fe-18 a/o Be alloy aged at 400°C for 1/2 hour, within the α + B2 metastable miscibility gap exhibited {100} modulations. The microstructure is indicative of a continuous decomposition of the ordered phase tending to produce a disordered α phase and an ordered B2 phase of different composition. The formation of this structure was accompanied by satellite reflections. The Fe-18 a/o Be alloy aged at 480°C is apparently just inside the spinodal which in this alloy is close to the B2 ordering transition (97). During phase separation at 480°C the Fe-rich regions disorder and the degree of order in the Be-enriched regions increases. Quenching to room temperature from the aging temperature produced a microstructure which when imaged in dark field exhibited fine bands of relatively dark and bright regions. The direct quenching and double aging experiments of Higgins et al. (100) produced some important results which are entirely compatible with the metastable diagram depicted in Fig. 23. Specimens directly quenched at 480°C and held for 5-1/2 hours followed by 3 hours at 425°C revealed a structure in dark field consisting of two alternate ordered phases with small domains evident in both the Fe-rich and Be-enriched regions as shown in Fig. 24. Subsequent cooling to 425°C and aging caused the Fe-rich modulations to continuously order. Prolonged aging at the lower temperatures, however, allowed the spinodal reaction to proceed towards the metastable phase boundaries resulting in equilibrium between a disordered and an ordered phase. Again we see that the various mechanisms of continuous transformation (ordering and clustering) can be interpreted in terms of simple thermodynamic and kinetic principles which follow from the necessary free energy relationships and stability conditions compatible with the phase diagram.

In 1972 Delaey, Perkins and Massalski (101) called attention to the numerous "anomalous" contrast and diffraction effects often reported in studies of β-brass type alloys. It is now clear that many of these effects must stem from spinodal decomposition of the CsCℓ-type or B2 phase. More recently Wayman and coworkers (102-104) have analyzed the "basket-weave"

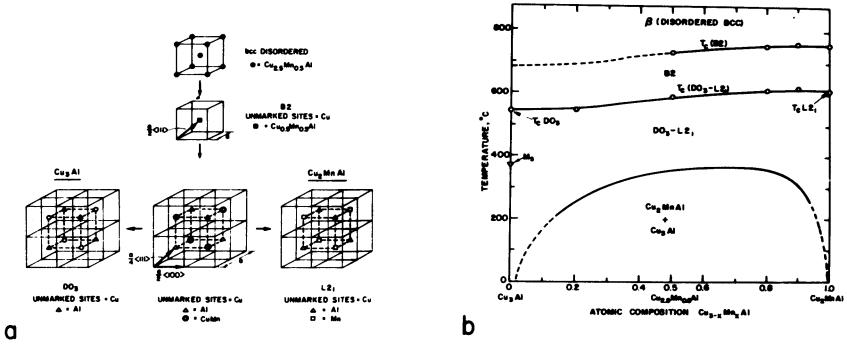

Fig. 21. (a) Schematic representation of the ordering sequence in the $Cu_{3-x}Mn_xA\ell$ alloys and phase separation, (b) phase diagram of the $Cu_{3-x}Mn_xA\ell$ alloys showing the ordering temperatures and miscibility gap (98).

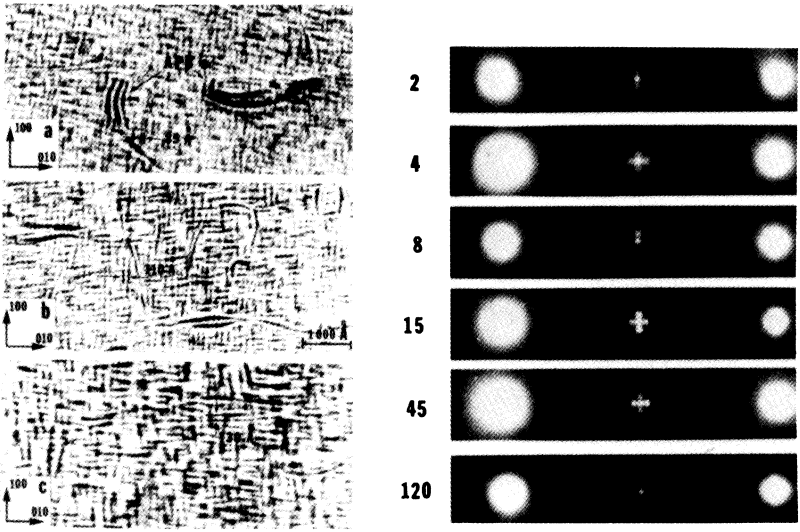

Fig. 22. Bright field electron micrographs from the spinodally decomposed $Cu_{2.2}Mn_{0.8}A\ell$ alloy aged for (a) 30 seconds, (b) 1 minute, (c) 2 minutes at 200°C showing the gradual increase in the wavelength of the modulated structure; $\vec{g}$ = 220. Diffraction patterns show satellites flanking superlattice reflections during aging at 200°C for times indicated (98).

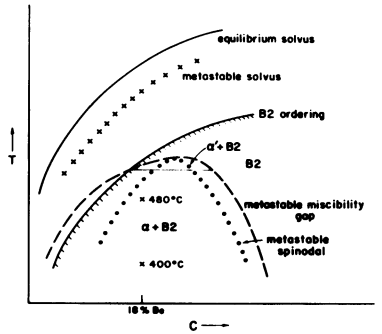

Fig. 23. Schematic depicting metastable order-disorder reaction and miscibility gap in the Fe-Be system.

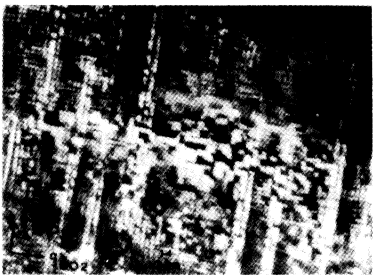

Fig. 24. Ordered domains in both Fe-rich and Be-rich modulations in spinodally decomposed Fe-Be alloy (100).

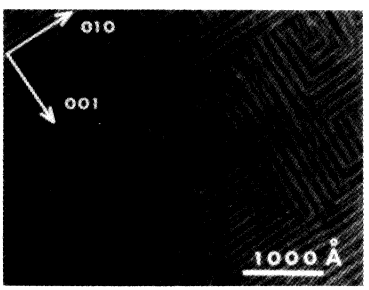

Fig. 25. Domains of one-dimensional spinodal lamellae in decomposed β-brass (104).

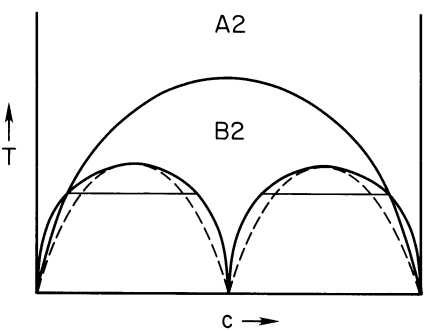

Fig. 26. Miscibility gaps at low temperatures intersecting the A2→B2 transition.

microstructure in thin foils of Cu-Zn alloys, and have interpreted these fine-scale precipitate structures in terms of spinodal decomposition of the ordered phase using an analysis similar to Richards (94) and Ino (97). Although substantially different types of diffuse scattering and satellite reflections appear in the diffraction patterns, Kubo et al. have shown that one set definitely derives from a modulated structure which forms at low temperatures. In the Cu-Zn alloys the spinodal reaction shown in Fig. 25 occurs only in thin foils and not in the bulk with one-dimensional lamellae or modulations developing in the thinnest regions of the specimen. Furthermore, the reaction is highly dependent on foil orientation. The variations in morphology and orientation dependence are explained in terms of the influence of the strain energy on the spinodal process. For example, the orientation dependence of the strain energy attendant to the phase separation suppresses decomposition in the "hard" {110} and {111} foils, but not in the elastically "soft" {100} foils. Spinodal decomposition of the ordered alloy can be readily understood in terms of the phase diagram shown in Fig. 26. This scheme, indicating phase separation of the ordered B2 phase, was applied specifically by Ino (97) to the Fe-Be system discussed earlier.

Closure

It is clear from this review that continuous decomposition or transformation involving clustering and/or ordering occurs in a wide variety of metallic alloy systems. Above all, this survey demonstrates the point that clustering and ordering are not mutually exclusive processes, but often occur together in a cooperative or interdependent manner during transformation. The construct of concentration waves proves to be a very useful tool for describing continuous phase separation and ordering, particularly in providing a link between the atomic rearrangements occurring and the attendant diffuse scattering effects in reciprocal space. The synergistics of clustering and ordering reactions in governing the microstructure resulting from precipitation is of great importance, since in the majority of commercial precipitation hardening systems the dispersed phase is a coherent, metastable ordered phase. Finally, we see that rather simple thermodynamic and kinetic principles combined with the phase diagram can provide a powerful tool for predicting the various possible reaction paths and mechanisms of phase transformation which control the morphology of the transformation products.

Acknowledgements

We would like to thank the National Science Foundation for continuing support of our research programs over the past several years. Also, we extend our sincere appreciation and recognition of the research efforts of our graduate students at the University of Pittsburgh and Carnegie-Mellon University. Furthermore, we wish to express our gratitude and appreciation to our colleagues and coworkers around the world, whose contributions have greatly extended our understanding of continuous transformations, and on whose works this review stands. Finally, we thank specifically our colleagues who have granted us permission to use their micrographs and figures in the paper.

This manuscript was prepared under the current sponsorship of The National Science Foundation Grants DMR80-05989/DMR80-22225 at the University of Pittsburgh and DMR78-05723-DMR81-05090 at Carnegie-Mellon University.

References

1. J. W. Gibbs, Scientific Papers, Vol. 1, Dover, New York (1961).
2. J. W. Christian, The Theory of Transformations in Metals and Alloys, Pergamon Press, Oxford (1975).
3. John W. Cahn, Acta Met. 9, 795 (1961).
4. John W. Cahn, Acta Met. 10, 179 (1962).
5. D. de Fontaine, Acta Met. 23, 553 (1975).
6. David E. Laughlin and John W. Cahn, Acta Met. 23, 329 (1975).
7. A. Datta and W. A. Soffa, Acta Met. 24, 987 (1976).
8. D. E. Laughlin, Acta Met. 24, 53 (1976).
9. A. J. Watts and B. Ralph, Acta Met. 25, 1013 (1977).
10. D. E. Laughlin, R. Sinclair and L. E. Tanner, Scripta Met. 14, 373 (1980).
11. M. Hillert, Acta Met. 9, 525 (1961).
12. M. Hillert, Sc.D. Thesis, Massachusetts Institute of Technology (1956).
13. John W. Cahn, Acta Met. 10, 907 (1962).
14. H. E. Cook, D. de Fontaine and J. E. Hilliard, Acta Met. 17, 765 (1969).
15. H. E. Cook and D. de Fontaine, Acta Met. 17, 915 (1969); 19, 607 (1971).
16. M. A. Krivoglaz, Theory of X-ray and Thermal Neutron Scattering by Real Crystals, Plenum Press, N.Y. (1969).
17. A. G. Khachaturyan, Progr. in Mater. Sci. 22, 1 (1978).
18. P. C. Clapp and S. C. Moss, Phys. Rev. 142, 418 (1966).
19. S. C. Moss and P. C. Clapp, Phys. Rev. 171, 754, 764 (1968).
20. D. de Fontaine, Met. Trans. 12A, 559 (1981).
21. H. E. Cook, Mater. Sci. and Engr. 25, 127 (1976).
22. V. Daniel and H. Lipson, Proc. Roy. Soc. London, Series A, 181, 368 (1943), 182, 378 (1944).
23. J. E. Hilliard in Phase Transformations, ASM, 497 (1970).
24. J. W. Cahn, Trans. TMS-AIME 242, 166 (1968).
25. D. de Fontaine in Ultrafine-Grain Metals (edited by J. J. Burke and V. Weiss), Syracuse University Press, Syracuse, N. Y. (1970).
26. A. J. Ardell and R. B. Nicholson, Acta Met. 14, 1295 (1966).
27. R. B. Nicholson and P. J. Tufton, Z. Angew. Phys. 21, 59 (1966).
28. E. P. Butler and G. Thomas, Acta Met. 18, 347 (1970); R. Livak and G. Thomas, Acta Met. 19, 497 (1971).
29. J. Manenc, Acta Met. 6, 145 (1958).
30. F. A. Badia, G. N. Kirby and J. R. Mihalisin, Trans. ASM 60, 395 (1967).
31. J. R. Mihalisin, E. L. Huston and F. A. Badia, Second International Conference on the Strength of Metals, Vol. II, 679, ASM (1970).
32. H. Kreye and P. Pech, Z. Metallkde. 64, 765 (1973).
33. J. E. Morral and J. W. Cahn, Acta Met. 19, 1073 (1971).
34. J. E. Morral, Acta Met. 20, 1061, 1069 (1972).
35. D. de Fontaine, J. Phys. Chem. Solids, 33, 297 (1972).
36. C. K. Wu and G. Thomas, Met. Trans. 8A, 1911 (1977).
37. A. Chou, A. Datta, G. H. Meier and W. A. Soffa, J. Mat. Sci. 13, 541 (1978).
38. C. K. Wu, R. Sinclair and G. Thomas, Met. Trans. 9A, 381 (1978).
39. R. Sinclair, R. Gronsky and G. Thomas, Acta Met. 24, 789 (1976).
40. B. Ditchek and L. H. Schwartz, Ann. Rev. Mater. Sci. 9, 219 (1979).
41. C. Bückle and J. Manenc, C.R. Acad. Sci. Paris, 244, 1643 (1957).
42. C. Bückle, B. Genty and J. Manenc, Rev. Met. 56, 247 (1959).
43. J. Manenc, Acta Met. 7, 124 (1959).
44. K. Saito and R. Watanabe, Jap. J. Appl. Phys. 8, 14 (1969).
45. R. Sinclair, J. A. Leake and B. Ralph, Phys. Status Solidi, 264, 285 (1974).
46. D. H. Ben Israel and M. E. Fine, Acta Met. 11, 1051 (1963).
47. S. L. Sass and J. B. Cohen, Trans. Met. Soc. AIME, 245, 153 (1969).

48. S. Allen and J. W. Cahn, Acta Met. 24, 425 (1976).
49. M. B. Thompson and J. W. Edington, Proceedings of 7th International Congress of Electron Microscopy, Grenoble, Vol. 2, 545 (1970).
50. J. W. Shilling and W. A. Soffa, Acta Met. 26, 413 (1978).
51. J. Singh, S. Lele and S. Ranganathan, J. Mat. Sci. 15, 2010 (1980).
52. S. A. Hill and B. Ralph, Proc. Conf. Phase Transformations, York, Inst. Metallurgists Conf. Ser. 3, No. 11, 2 44 (1979).
53. C. Bückle and J. Manenc, Mem. Sci. Rev. Met. 57, 435 (1960).
54. T. Hakkarainen, Doctoral Thesis, Helsinki University of Technology, Helsinki (1971).
55. J. A. Cornie, A. Datta and W. A. Soffa, Met. Trans. 4, 727 (1973).
56. R. Knights and P. Wilkes, Acta Met. 21, 1503 (1973).
57. D. E. Laughlin and J. W. Cahn, Scripta Met. 8, 75 (1974).
58. D. E. Laughlin and J. W. Cahn, Met. Trans. 5, 972 (1974).
59. K. E. Biehl and R. Wagner, 27th Field Emission Symposium, Japan, p 267 (1980).
60. T. Tsujimoto, K. Hashimoto and K. Saito, Acta Met. 25, 295 (1977).
61. M. E. Hargreaves, Acta Cryst. 301, 4 (1951).
62. D. Balli and M. Zakharova, Dakl. Akad. Nauk USSR, 96, 453, 737 (1954).
63. T. J. Tiedema, J. Boumann and W. G. Burgers, Acta Met. 5, 310 (1957).
64. E. Biedermann, Acta. Cryst. 13, 650 (1960).
65. A. Guinier, Acta Met. 3, 510 (1955).
66. Yu. D. Tiapkin and M. V. Jibuti, Acta Met. 19, 365 (1971).
67. L. H. Schwartz, S. Mahajan and J. T. Plewes, Acta Met. 22, 601 (1974).
68. S. Spooner and B. G. Lefevre, Met. Trans. 11A, 1085 (1980).
69. B. Ditchek and L. H. Schwartz, Acta Met. 28, 807 (1980).
70. L. H. Schwartz and J. T. Plewes, Acta Met. 22, 911 (1974).
71. T. Tsakalakos and J. E. Hilliard, to be published.
72. P. R. Okamoto and G. Thomas, Acta Met. 19, 825 (1971); P. R. Okamoto, Ph.D. Thesis, U. of California, Berkeley, UCRL-19175 (1970).
73. D. de Fontaine, Solid State Physics, H. Ehrenreich, F. Seitz and D. Turnbull, eds. 34, 73 (1979).
74. L. A. Nesbit and D. E. Laughlin, Acta Met. 26, 815 (1978).
75. T. Saburi, E. Kanai and S. Nenno, J. of the Less-Common Metals, 37, 59 (1974).
76. H. Chen and J. B. Cohen, Acta Met. 27, 603 (1979).
77. P. E. J. Flewitt, Acta Met. 22, 47 (1974).
78. C. Cousdone, P. S. Ho and S. L. Sass, Acta Met. 20, 432 (1972).
79. E. Hornbogen, G. Lutjering and M. Roth, Arch. Eissenhutt. 37, 523 (1966).
80. J. Higgins and P. Wilkes, Phil. Mag. 25, 599 (1972).
81. T. Miyazaki, S. Takagishi, H. Mori and T. Kozakai, Acta Met. 28, 1143 (1980).
82. R. M. Fisher, E. J. Dulis and K. G. Carroll, Trans. AIME, 197, 690 (1953).
83. R. O. Williams and H. W. Paxton, J. Iron Steel Inst. 185, 358 (1957).
84. R. O. Williams, Trans. TMS-AIME, 212, 497 (1958).
85. R. Lagnesborg, Trans. ASM, 60, 67 (1967).
86. T. J. Nichol, A. Datta and G. Aggen, Met. Trans. 11A, 573 (1980).
87. D. Chandra and L. H. Schwartz, Met. Trans. 2, 511 (1971).
88. T. DeNys and P. M. Gielen, Met. Trans. 2, 1423 (1971).
89. S. Brenner, D. Miller and W. A. Soffa, this conference.
90. J. W. Cahn and R. J. Charles, Phys. Chem. Glasses, 6, 181 (1965).
91. S. Jin, S. Mahajan and D. Braen, Met. Trans. 11A, 69 (1980).
92. M. Okada, G. Thomas, M. Homma and H. Kaneko, IEEE Trans. Mag. 14, 245 (1978).
93. R. B. Griffiths, J. Chem. Phys. 60, 195 (1974).
94. M. J. Richards, Sc.D. Thesis, M.I.T. Cambridge, MA (1971).
95. M. J. Richards and J. W. Cahn, Acta Met. 19, 1263 (1971).

96. M. Hasaka, Trans. J.I.M. 21, 660 (1980).
97. H. Ino, Acta Met. 26, 827 (1978).
98. M. Bouchard and G. Thomas, Acta Met. 23, 1485 (1975).
99. R. M. Richman and R. G. Davies, Trans. AIME, 236, 1551 (1966).
100. J. Higgins, R. B. Nicholson and P. Wilkes, Acta Met. 22, 201 (1974).
101. L. Delaey, A. J. Perkins and T. B. Massalski, J. Mat. Sci. 7, 1197 (1972).
102. H. Kubo and C. M. Wayman, Met. Trans. 10A, 633 (1979).
103. H. Kubo and C. M. Wayman, Acta Met. 28, 395 (1980).
104. H. Kubo, I. Cornelis and C. M. Wayman, Acta Met. 28, 405 (1980).

Note Added in Proof

Cockayne and Gronsky have addressed this problem specifically for the case of modulated structures in a recent paper. See Phil. Mag. A 44, 159 (1981).